16th World Conference on Earthquake, 16WCEE 2017
Santiago Chile, January 9th to 13th 2017
Paper N° 635 (Abstract ID)
Registration Code: S-W1464620396

EFFECTS OF ARTIFICIAL PULSE-TYPE GROUND MOTIONS ON SUPER-SPAN CABLE-STAYED BRIDGE SYSTEMS

F. Zhang (1), S. Li (2), J.Q. Wang(3)

(1) *Ph.D. Candidate, Key Laboratory of Concrete and Prestressed Concrete Structure of China Ministry of Education, Southeast University, Nanjing 210096, China. E-mail: reallyreallyfan@vip.qq.com*
(2) *Ph.D. Candidate, Key Laboratory of Concrete and Prestressed Concrete Structure of China Ministry of Education, Southeast University, Nanjing 210096, China. E-mail: hmlishuai@163.com*
(3) *Associate Professor, Key Laboratory of Concrete and Prestressed Concrete Structure of China Ministry of Education, Southeast University, Nanjing 210096, China. (corresponding author). E-mail: wangjignquan@seu.edu.cn*

Abstract

The focus of this paper is to determine the seismic response of a super-span cable-stayed bridge subjected to near-fault ground motions. Here, a new method called "record decomposition-incorporation" (RDI) has been proposed to synthesize the artificial near-fault pulse-type ground motions by combining the high-frequency Background Record (BGR) with simple equivalent pulses. The Sutong Cable-stayed Bridge (SCB) in China, with a main span of 1088 m, is taken as an example. The results show that the high-frequency components of near-fault records have a significant effect on the response of the bridge, and the artificial ground motions can capture the important response characteristics of the near-fault records. When FD records have the same PGV with FS records, the former records result in greater deformation demands than the latter, whereas the latter may result in greater strength demands. The PGVs of near-fault records exhibit obvious correlations with the seismic responses of the tower. The fling-step records with different pulse periods generate larger deformations and increase demands on the bridge compared to the forward-directivity records.

Keywords: near-fault ground motion, pulse model, forward-directivity effect, fling-step effect, cable-stayed bridge

1. Introduction

Near-fault ground motions often possess distinct characteristics that make them different from those recorded in far-fault regions and can have strong influences on the structural response, especially for long-period structures [1-3]. Such effects include the forward directivity effect in the fault-normal (FN) direction and the fling-step effect in the fault-parallel (FP) direction [4]. Due to these two effects, near-fault ground motion usually exhibits two important characteristics: a pulse-like velocity waveform and a permanent ground displacement, which may generate high demands that will force the structures to dissipate large amount of input energy with few large displacement excursions. Additionally, the high-frequency content portion is another important specification in the near-fault ground motions because the short travel distance of the seismic waves prevents them from being damped, as observed in the case of far-field records [5]. The above-mentioned characteristics have attracted much attention as important research topics in engineering communities. However, the influence of records with different pulse types on structural response has not been well understood [6-8]. Additionally, numbers of near-fault records with pulse effect are scarce (Only 142 stations have recorded the pulse-type ground motions from the latest database of the PEER Next Generation Attenuation phase 2 (PEER NGA-West 2)). Obviously, it is necessary to extensively examine the effects of two types of impulsive ground motions with different pulse parameters (i.e., pulse duration and velocity amplitude) on the response of structures, especially on important long-period life-line structures.

To quantify the pulse-type effects, a large effort has been focused on presenting synthetic simplified models to simulate these pulse-type ground motions [9-11]. Other researchers have used equivalent pulse models to represent real near-fault records to study the seismic response of structures [12]. However, the simplified models that are representing the near-fault ground motions do not contain the high-frequency content portion that may play an important role for short-period and long-period structures in which higher modes are significant. To efficiently represent the near-fault ground motions, Baker used wavelet analysis to decompose the real recordings into the main pulses and residual records [13]. Based on Baker's method, only the main pulse can be extracted, and the remaining low-frequency components are allocated to residual records. Ghahari et al. proposed an improved method [5]. He used a moving average filter (MAF) to decompose the near-fault records into a Pulse-type Record (PTR) and Background Record (BGR). The MAF can consider low-frequency components as a part of the PTR, which leads to an almost purely high-frequency BGR. Although both methods can extract different components to accurately evaluate the seismic response of structures, the procedures for generating synthetic near-fault ground motions with different pulse parameters are not available to design engineers. The recent work of Yan et al. [14] presented a synthetic method developed by combining the real near-field non-pulse ground motion with simple equivalent pulses. Using this method, the effects of the velocity pulses and high-frequency components of the near-field site can be considered. Because near-fault recordings exhibit substantial variations (i.e., radiation pattern, rupture mechanism, and geomorphology) in the vicinity of an active fault system, considering real non-pulse records as fully representative of the high-frequency content portions in the pulse-type records causes the differences in the spectrum characteristics.

The effects of near-fault ground motion on short-period bridges and bents have been investigated in many recent studies [15-19]. However, for long-period life-line structures, e.g., long-span bridges, it is critical to understand the effects of pulse-type ground motions and its associated hazard under such type ground motions for seismic evaluation purposes. Some studies have focused on the seismic response of long-period structures under near-fault records with pulse-type effects [20-23]. It is clear from these studies that the near-fault ground motion effect on the response of long-period bridges requires careful consideration. Unfortunately, there is insufficient research on this topic, in particular the different effects of the fling-step pulses and forward-directivity pulses of near-fault ground motions on the responses of long-period bridges.

The main objective of this paper is to investigate the different effects of near-fault ground motions with forward directivity and fling step on the seismic response of long-period bridge structures. A new method for synthetic ground motions called "record decomposition-incorporation" (RDI) has been developed by combining the high-frequency Background Record (BGR) of real pulse-type records with simple equivalent pulses. The Sutong Cable-stayed Bridge (SCB), which is the second-longest cable-stayed bridge in the world, with a main span of 1088 m, is taken as a case study. It can be proved that RDI method can capture the important characteristics and natural variability of recorded near-fault ground motions. Subsequently, the effects of the pulse parameters of near-fault ground motions on the response of the bridge are systematically discussed.

2. RDI method of synthetic artificial pulse-type ground motions

In this paper, as an alternative to current approaches, a new method called the "record decomposition-incorporation" (RDI) of synthetic pulse-type ground motions has been developed by combining the high-frequency Background Record (BGR) of real pulse-type records with simple equivalent pulses.

2.1 Record decomposition

A fourth-order Butterworth filter is used to decompose near-fault pulse-type ground motions into 2 components (A and B) having different frequency contents: a) component A, denoted here as Background Record (BGR), is a relatively high-frequency record, and b) component B is a low-frequency part of the record Pulse-Type Record (PTR). The velocity time history of the ground motion is expressed as Eq. 1,

$$v_g(t) = v_{g,BGR}(t) + v_{g,PTR}(t) \tag{1}$$

in which $v_g(t)$ is the velocity time history of the near-fault records, $v_{g,BGR}(t)$ is the high-frequency part without pulses, and $v_{g,PTR}(t)$ is the low-frequency pulse-type part of the velocity time history.

The Butterworth filter is referred to as a maximally flat magnitude filter and is commonly used for strong motion data processing such as that conducted by the United States Department of the Interior Geological Survey (USGS), California Strong Motion Instrumentation Program and PEER. The frequency response of this filter is as follows:

$$H(f)=\frac{1}{1+\left(\frac{f}{f_c}\right)^{2n}} \tag{2}$$

in which f_c is the filter's cut-off frequency and n is the number of the order.

A key part of Butterworth filtering is defining the appropriate filter cut-off frequency. When the value of f_c is high, the artificial ground motions may miss important high-frequency components. Conversely, when the value of f_c is low, the pulse characteristics of the PTR may be not prominent. Here, the effective cut-off frequency is calculated as follows:

$$f_c=\frac{1}{\alpha T_p-dt} \tag{3}$$

in which dt is the length of the time intervals in the input signal, T_p is the period of the dominant pulse in the velocity time history, and α is an empirical coefficient. The empirical coefficient of the fling-step ground motion is set to 0.25, which is the same as that suggested by Ghahari. Because the pulse characteristics of the fling-step records differ from those of the forward-directivity records, pseudo-velocity response spectra of the original records with forward-directivity effects conducted by Ghahari do not agree well with that of the pulse-type components in the long-period range. Hence, the coefficient of the records with forward-directivity effects should be re-examined. In this paper 20 records with forward-directivity effect are selected from PEER database. The value of α for each record is determined. Then, according to the values, the mean value of 0.8 is calculated and set as the suggested value of α for the records with forward-directivity effect.

2.2 Synthetic ground motions based on RDI

As mentioned above, there are a substantial number of simplified pulse models that attempt to capture the important characteristics of recorded near-fault ground motions. Mavroeidis and Papageorgiou proposed an equivalent pulse model of velocity that could be used to analyze the effects of pulse parameters on the response of structures. The mathematical model is given by the following equation:

$$v(t)=\begin{cases} A\frac{1}{2}[1+\cos(\frac{2\pi f_p}{\gamma}(t-t_0))]\cos[2\pi f_p(t-t_0)+\varphi], t_0-\frac{\gamma}{2f_p}\le t\le t_0+\frac{\gamma}{2f_p}, \gamma>1 \\ 0, otherwise \end{cases} \tag{4}$$

in which $v(t)$ is the artificial velocity time history; A and f_p are the amplitude and prevailing frequency of the signal, respectively; t_0 specifies the time of the envelope's peak; φ is the phase of the amplitude-modulated harmonic; and γ is the oscillatory character parameter. The parameters φ and γ can be used to define the pulse shape, i.e., $\varphi=0$ and $\varphi=\pm\frac{\pi}{2}$ define symmetric and antisymmetric signals, and γ defines the number of zero crossings.

The Mavroeidis model is used to simulate the PTR of actual near-fault records, and the simple pulse is denoted here as Artificial Pulse-type Motion (APT). More details about the procedure can be seen in Mavroeidi's paper. The artificial near-fault records (ANRs) are synthesized by combing the BGR with the APT, which is expressed as Eq. 5.

$$v_{g,ANR}(t)=v_{g,BGR}(t)+v_{g,APT}(t) \tag{5}$$

in which $v_{g,ANR}(t)$ is the artificial velocity time history, $v_{g,BGR}(t)$ is the BGR of the actual record, and $v_{g,APT}(t)$ is the artificial pulse-type part.

2.3 Validation of the RDI method

In order to validate the effectiveness of the above method, 2 actual records with different pulse effects (E04-230 and ARE-090) are taken as examples. The input parameters obtained by fitting the Mavroeidis model to the recorded ground motions are summarized in Table 1.

The artificial velocity time histories based on the proposed method are illustrated in Fig. 1. The pulses extracted by the Butterworth filter (PTR) along with the Artificial Pulse-type Motion (APT) extracted by the Mavroeidis model are shown on the left. Additionally, the original velocity and the artificial near-fault records (ANRs) are compared on the right. The Mavroeidis model captures the main pulses extracted by the Butterworth filter, and the artificial near-fault records (ANRs) are in good agreement with the original velocity. However, using the Mavroeidis model may cause the remaining low-frequency components to be ignored. The pseudo-acceleration and pseudo-velocity response spectra for the records of Fig. 1 are presented in Fig. 2. Fig. 2 reveals that the frequency content of the corresponding original records and the ANRs are consistent and that the ANRs can capture the essential response characteristics of the near-fault records.

Table 1 – Model input parameters

Ground motions	**Station, component**	**A**	T_p	φ	γ	t_0
Forward-directivity pulses	E04-230	-66.2	4.8	140	2	7.85
Fling-step pulses	ARE-090	-33.1	7.7	225	1.5	15.5

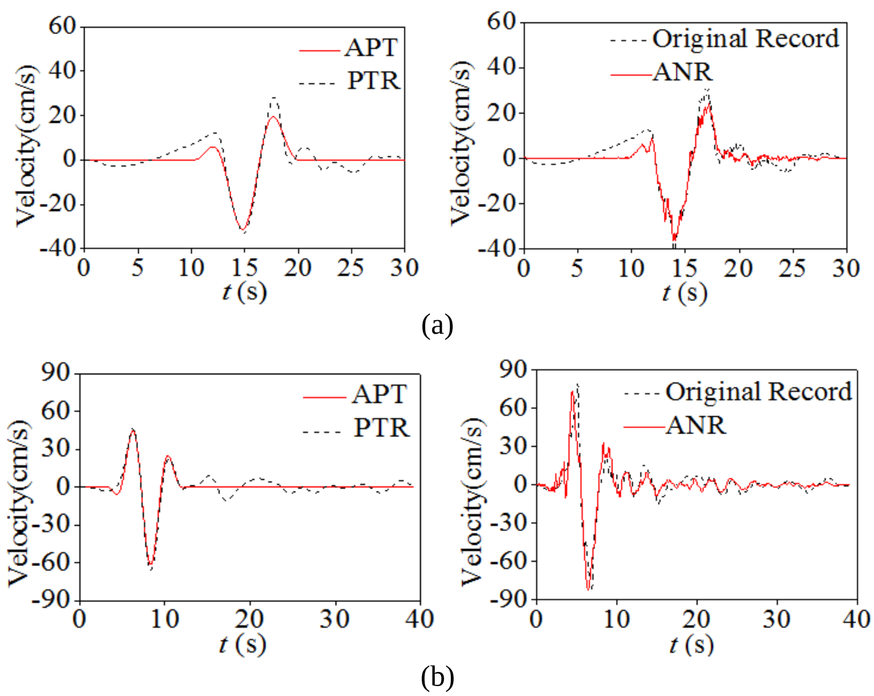

Fig. 1 – Examples of near-fault records: (a) ARE-090; (b) E04-230. In each part: Left: the pulses extracted by the Butterworth filter (PTR) and the Artificial Pulse-type Motion (APT) simulated by the Mavroeidis model. Right: the original velocity time histories and the artificial near-fault records (ANRs)

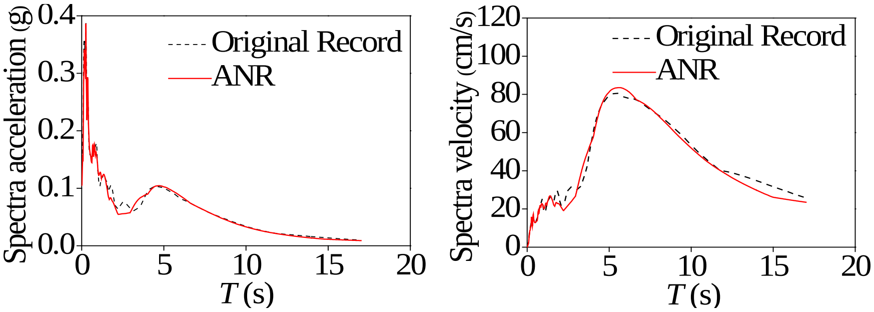

(a)

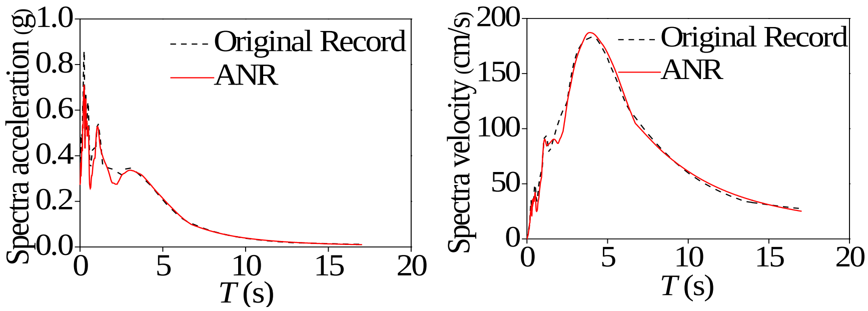

(b)

Fig. 2 – Comparison of pseudo-acceleration (pseudo-velocity) response spectra of the original records and the artificial near-fault records (ANRs): (a) ARE-090; (b) E04-230. Left: pseudo-acceleration response spectra. Right: pseudo-velocity response spectra

3. Response of the SCB to the synthetic artificial ground motions

To investigate the response of long-period bridge structures, a case study that utilized the Sutong Cable-stayed Bridge (SCB) as a representative long-span bridge is performed (Fig. 3). This bridge connects Suzhou and Nantong City. It is the second-longest cable-stayed bridge in the world, with a main span of 1088 m. A streamlined flat steel box girder is employed as the deck, and the overall width is 41.0 m. Two inverted-Y pylons with a total height of 300.4 m are used to support the bridge. The stay cables, with intervals of 16 m on the deck and 2 m on the towers, are arranged in a fan configuration, and a total of 272 cables are used. In order to improve the rigidity of the side span and to carry the forces mainly generated by live loads, two auxiliary piers are constructed on each side span. The counterweights in the two side spans are applied to balance the weight of the main span. The configuration of the bridge is presented schematically in Fig. 4.

Fig. 3 – Sutong Cable-stayed bridge

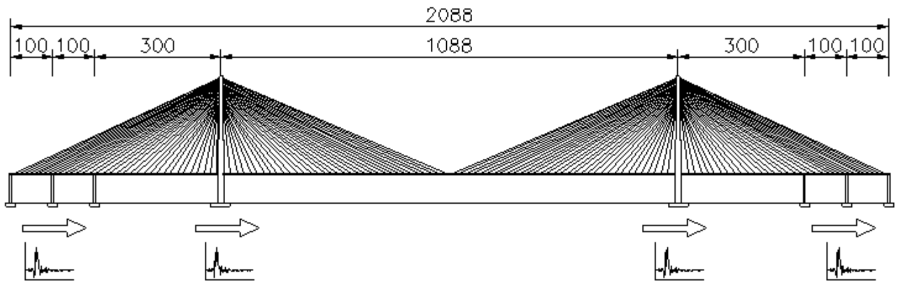

Fig. 4 – Elevation configuration of the SCB (meters)

A three-dimensional (3D) finite element (FE) model of the bridge is constructed to represent the full structural system. The FE model is created using a commercial software ANSYS (Release 14 2012). A detailed description of the model is given as follows. The towers, piers, steel girders, and transverse diaphragms are modeled using two-noded beam elements (Beam 4 in ANSYS). The girders are discretized based on the suspended points of the stayed cables. The cables are modeled with 3D tension-only truss elements (Link 10), and the nonlinearity of the inclined stayed cables due to gravity is considered with the Ernst equation of equivalent modulus of elasticity [25]. The translational degrees of piers and transverse diaphragms are coupled in the vertical and transverse directions where both the towers and piers are considered to be fixed to their foundations. The first natural frequency is 0.061 Hz, i.e. the period is 16.4 sec, and the corresponding mode is the longitudinal floating vibration. The wave-passage effect and soil-structure interaction effect are ignored in this study.

Two records are taken as examples to re-examine the proposed method in seismic response evaluation: TCU052-NS (Chi-Chi) with the fling-step effect and TCU054-EW (Chi-Chi) with the forward-directivity effect. The seismic response along the height of the SCB tower subjected to the actual records, artificial ground motions based on the proposed method, the pulses (PTR) extracted by Butterworth filtering and the equivalent pulses based on the Mavroeidis model are compared. Based on the linear scaling, the PGAs of the actual records are scaled to a peak value of 0.3g for the analysis.

Fig. 6 demonstrates the importance of the high-frequency components of the near-fault records in seismic response evaluation. It is apparent that the seismic response of the tower under the PTR and equivalent pulses is smaller than that when subjected to the original records and artificial records. The displacement and moment responses of the SCB tower subjected to the artificial records agree well with those of the tower subjected to the actual records.

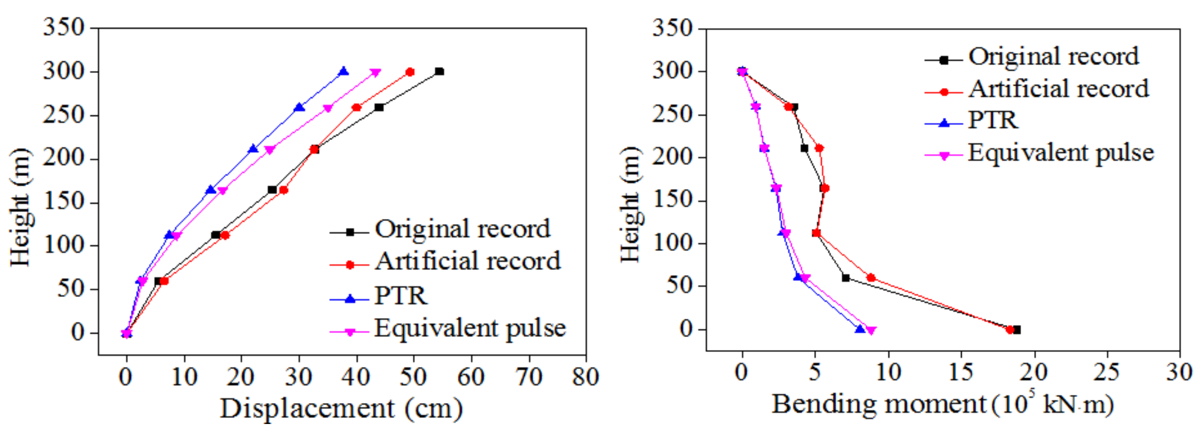

(a)

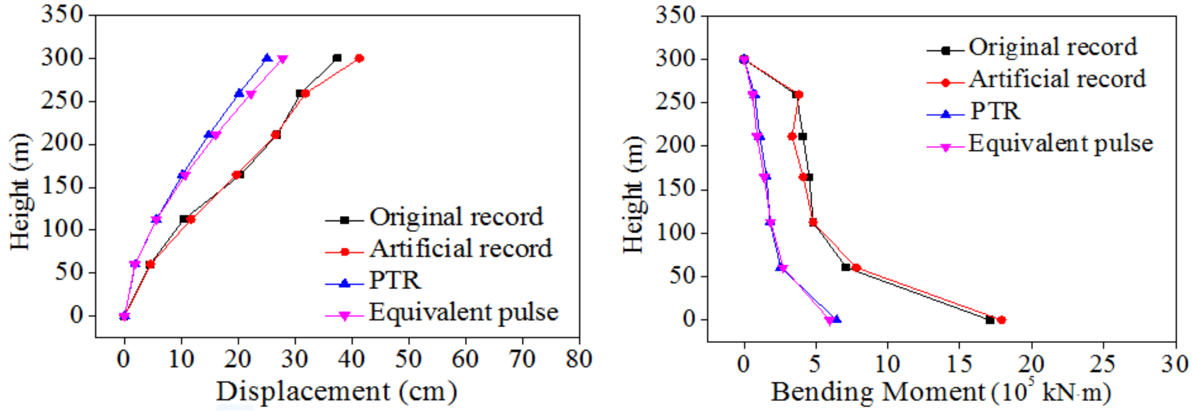

(b)

Fig. 6 – Seismic response comparison of the SCB tower: (a) Fling-step motions; (b) Forward-directivity motions

4. Effects of pulse parameters on the seismic response of the SCB

Based on the above-mentioned RDI method, artificial near-fault pulse-type ground motions can be generated to facilitate the investigation of the effects of pulse parameters associated with near-fault pulse-type ground motion on the response of the SCB. The high-frequency components of TCU052-NS and TCU054-EW (Chi-Chi) are chosen as the BGRs of the artificial ground motions.

4.1 Effects of pulse velocity amplitude on the dynamic response of SCB

Fig. 7 and Fig. 8 illustrate the seismic response of the SCB tower subjected to artificial ground motions with different PGV amplitudes. It should be noted that the period of the equivalent velocity pulses is the same as that of the PTR of TCU052-NS and TCU054-EW.

The figures show that the seismic responses of the SCB tower subjected to two types of impulsive motions increase with increasing velocity amplitude. Furthermore, comparing the response of the tower subjected to two types of impulsive ground motions, the displacements of the tower induced by the forward-directivity ground motions are larger than those induced by fling-step ground motions; however, the bending moments caused by the former are smaller than those caused by the latter. Additionally, it is apparent that the deformation of the tower subjected to fling-step pulses with different velocity amplitudes display significant differences. Higher mode effects are not as evident in the response to fling-step motions with high velocity amplitudes, but they are more clearly evident for fling-step motions when the PGV is less than 100 cm/s. In addition, records with the forward-directivity effect caused the tower to respond primarily in the lower modes.

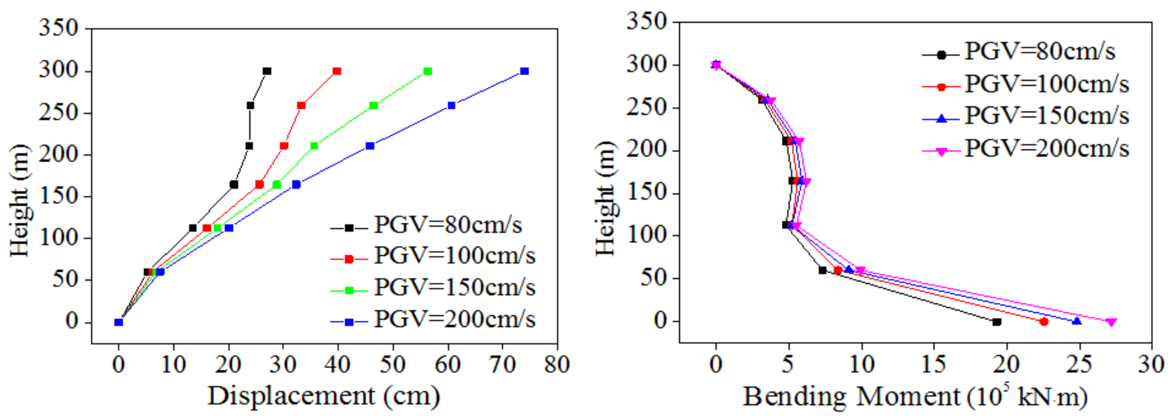

(a) (b)

Fig. 7 – The dynamic response of the SCB to artificial fling-step pulses with different velocity amplitudes: (a) the longitudinal displacement; (b) the bending moment

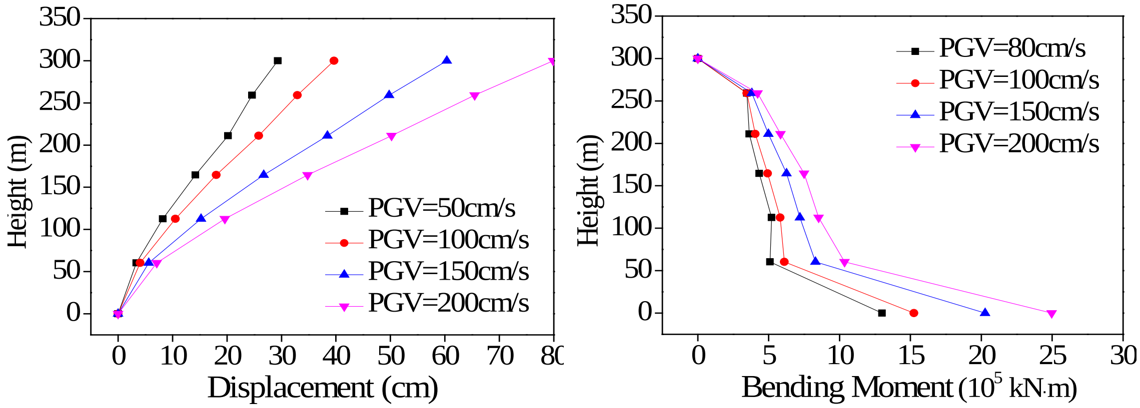

(a) (b)

Fig. 8 – The dynamic response of the SCB to artificial forward-directivity pulses with different velocity amplitudes: (a) the longitudinal displacement; (b) the bending moment

4.2 Effects of pulse periods on the dynamic response of SCB

The bridge model is re-analyzed using artificial ground motions with forward-directivity and fling-step effects to study the influence of the pulse period on the seismic response. In this case, the velocity amplitudes of equivalent pulses correspond to the PGV of the PTR extracted from the actual records, and the pulse period (T) is varied from 0.5 to 1.5 of the fundamental period (Tg) of the SCB. Fig. 9 and Fig. 10 illustrate the seismic response of the tower subjected to two types of impulsive motions with different pulse periods.

Fig. 9 shows that with increasing pulse period, the displacements of the tower induced by fling-step ground motions exhibit an increasing trend. For instance, the ground motion with long period (T_p/T=1.5) results in a displacement that is 23.1% larger compared to the short-period ground motion (T_p/T=0.5). Moreover, the bending moments of the tower increase with the pulse periods; however, the increasing trend is not apparent when Tp/T exceeds 0.8.

Fig. 10 shows that the displacement of the tower attains the minimum in the vicinity of the period T=Tp. Similar to section 7.1, forward-directivity pulses excite the fundamental mode of the main tower. However, the overall pulse period for forward-directivity ground motions has little correlation with the seismic response of the tower.

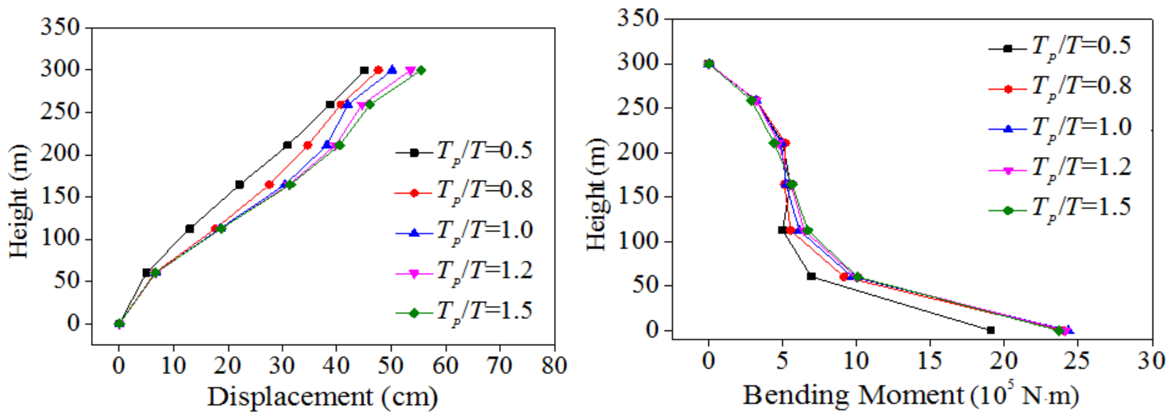

(a) (b)

Fig. 9. The dynamic response of the SCB to artificial fling-step pulses with different pulse periods: (a) the longitudinal displacement; (b) the bending moment

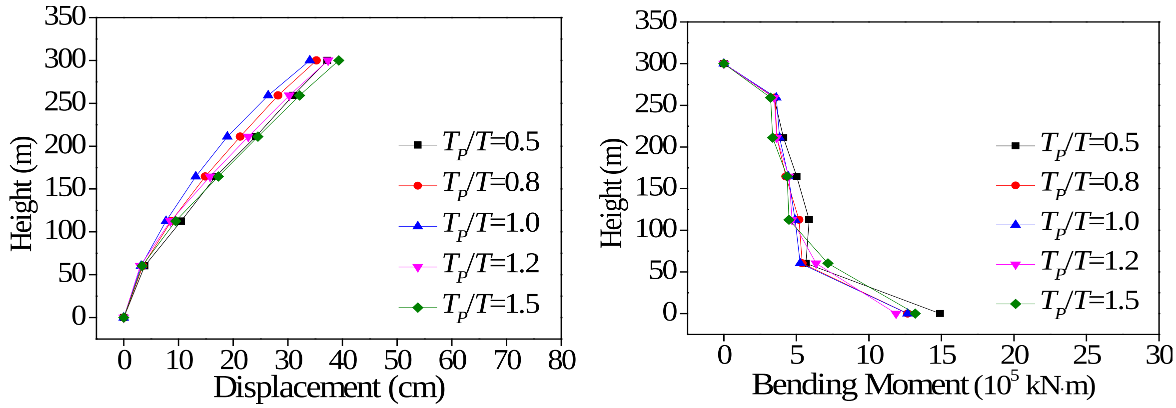

(a) (b)

Fig. 10. The dynamic response of the SCB to artificial forward-directivity pulses with different pulse periods: (a) the longitudinal displacement; (b) the bending moment

5. Conclusions

The seismic responses of the Sutong cable-stayed bridge (SCB) subjected to near-fault ground motions are examined here in this paper. A new method called "record decomposition-incorporation" (RDI) that synthesizes artificial near-fault pulse-type ground motions by combining the high-frequency Background Record (BGR) with simple equivalent pulses has been proposed. Furthermore, simple input pulses are synthesized to simulate artificial forward-directivity effects in ground motions originally having fling steps. The effects of near-fault ground motions with different pulse parameters on the response of the bridge are assessed. The conclusions of this study are summarized as follows:

1. The high-frequency Background Records (BGRs) of the near-fault ground motions have a significant effect on the seismic response. The RDI method can capture the essential response characteristics of the bridge subjected to near-fault ground motions.

2. When FD records have the same PGV with FS records, the former records result in greater deformation demands than the latter, whereas the latter may result in greater strength demands.

3. The deformation and internal force of the tower subjected to near-fault ground motions with different PGVs increase with the PGV of the near-fault pulse-type records. Records with fling-step effects, which have a low PGV/PGA, result in more instances of higher mode demand, and waveforms with forward directivity cause the towers to respond primarily in the lower mode.

6. Acknowledgements

This study was supported by National Natural Science Foundation of China (Grant No. 51378110), Graduate Student Research Innovation Project of Jiangsu Province (Grant No. KYLX15_0086) and Priority Academic Program Development of Jiangsu Higher Education Institutions (Grant No. CE02-2-6). The financial supports are greatly appreciated.

7. Copyrights

8. Reference

[1] Bray JD, Rodriguez-Marek A (2004): Characterization of forward-directivity ground motions in the near-fault region. Soil dynamics and earthquake engineering, 24(11), 815-828.

[2] Mortezaei A, Ronagh HR (2013): Plastic hinge length of reinforced concrete columns subjected to both far -fault and near -fault ground motions having forward directivity. The Structural Design of Tall and Special Buildings,22(12), 903-926.

[3] Sehhati R, Rodriguez MA, ElGawady M, Cofer WF (2011): Effects of near-fault ground motions and equivalent pulses on multi-story structures. Engineering Structures, 33(3), 767-779.

[4] Somerville PG, Smith NF, Graves RW, Abrahamson NA (1997): Modification of empirical strong ground motion attenuation relations to include the amplitude and duration effects of rupture directivity. Seismological Research Letters, 68(1), 199-222.

[5] Ghahari SF, Jahankhah H, Ghannad MA (2010): Study on elastic response of structures to near-fault ground motions through record decomposition. Soil dynamics and earthquake engineering, 30(7), 536-546.

[6] Yang D, Pan J, Li G (2010): Interstory drift ratio of building structures subjected to near-fault ground motions based on generalized drift spectral analysis. Soil Dynamics and Earthquake Engineering, 30(11), 1182-1197.

[7] Jiang Y, Yang D, Li G (2010): Effects of forward directivity and fling step of near-fault ground motions on seismic responses of high-rise steel structure. Jianzhu Jiegou Xuebao(Journal of Building Structures), 31(9), 103-110.

[8] Kalkan E, Kunnath SK (2006): Effects of fling step and forward directivity on seismic response of buildings. Earthquake spectra, 22(2), 367-390.

[9] Alavi B, Krawinkler H (2004): Behavior of moment-resisting frame structures subjected to near -fault ground Earthquake engineering & structural dynamics, 33(6), 687-706.

[10] Mavroeidis GP, Papageorgiou AS (2003): A mathematical representation of near-fault ground motions. Bulletin of the Seismological Society of America, 93(3), 1099-1131.

[11] He WL, Agrawal AK (2008): Analytical model of ground motion pulses for the design and assessment of seismic protective systems. Journal of Structural Engineering, 134(7), 1177-1188.

[12] Wu G, Zhai C, Li S, Xie L (2014): Effects of near-fault ground motions and equivalent pulses on Large Crossing Transmission Tower-line System. Engineering Structures, 77, 161-169

[13] Baker JW (2007): Quantitative classification of near-fault ground motions using wavelet analysis. Bulletin of the Seismological Society of America, 97(5), 1486-1501.

[14] Yan G, Chen F (2015): Seismic Performance of Midstory Isolated Structures under Near-Field Pulse-Like Ground Motion and Limiting Deformation of Isolation Layers. Shock and Vibration, 2015.

[15] Saiidi MS, Vosooghi A, Choi H, Somerville P (2013): Shake Table Studies and Analysis of a Two-Span RC Bridge Model Subjected to a Fault Rupture. Journal of Bridge Engineering, 19(8), A4014003

[16] Billah A, Alam M, Bhuiyan M (2013): Fragility Analysis of Retrofitted Multicolumn Bridge Bent Subjected to Near-Fault and Far-Field Ground Motion. Bridge Eng., 18(10), 992–1004.

[17] Liao WI, Loh CH, Lee BH (2004): Comparison of dynamic response of isolated and non-isolated continuous girder bridges subjected to near-fault ground motions. Engineering Structures, 26(14), 2173-2183.

[18] Gulerce Z, Erduran E, Kunnath SK, Abrahamson NA (2012): Seismic demand models for probabilistic risk analysis of near fault vertical ground motion effects on ordinary highway bridges. Earthquake Engineering & Structural Dynamics, 41(2), 159-175.

[19] Jalali RS, Jokandan MB, Trifunac MD (2012): Earthquake response of a three-span, simply supported bridge to near-field pulse and permanent-displacement step. Soil Dynamics and Earthquake Engineering,43, 380-397.

[20] McCallen D, Astaneh-Asl A, Larsen SC, Hutchings LJ (2009): The response of long-span bridges to low frequency, near-fault earthquake ground motions. In Proceedings of the 2009 Technical Conference on Lifeline Earthquake Engineering Am. Soc. of Civil Eng.

[21] Shrestha B (2015): Seismic response of long span cable-stayed bridge to near-fault vertical ground motions. KSCE Journal of Civil Engineering, 19(1), 180-187.

[22] Ismail M, Casas JR, Rodellar J (2013): Near-fault isolation of cable-stayed bridges using RNC isolator. Engineering Structures, 56, 327-342.

[23] Adanur S, Altunişik AC, Bayraktar A, Akköse M (2012): Comparison of near-fault and far-fault ground motion effects on geometrically nonlinear earthquake behavior of suspension bridges. Natural hazards, 64(1), 593-614.

[24] ANSYS Mechanical APDL 2012 Release 14.0 ANSYS Ltd.

[25] Ernst HJ (1965): Der E-Modul von Seilen unter berucksichtigung des Durchhanges. Der Bauingenieur, 40(2), 52-55.

[26] JTG/T B02-01-2008. Guidelines for Seismic Design of Highway Bridges.